AJNR

Intracranial-Derived Atherosclerosis Assessment: An In Vitro Comparison between Virtual Histology by Intravascular Ultrasonography, 7T MRI, and Histopathologic Findings

S. Majidi, J. Sein, M. Watanabe, A.E. Hassan, P.-F. Van de Moortele, M.F.K. Suri, H.B. Clark and A.I. Qureshi

AJNR Am J Neuroradiol 2013, 34 (12) 2259-2264
doi: https://doi.org/10.3174/ajnr.A3631
http://www.ajnr.org/content/34/12/2259

Intracranial-Derived Atherosclerosis Assessment: An In Vitro Comparison between Virtual Histology by Intravascular Ultrasonography, 7T MRI, and Histopathologic Findings

S. Majidi, J. Sein, M. Watanabe, A.E. Hassan, P.-F. Van de Moortele, M.F.K. Suri, H.B. Clark, and A.I. Qureshi

ABSTRACT

BACKGROUND AND PURPOSE: Atherosclerotic plaque composition and structure contribute to the risk of plaque rupture and embolization. Virtual histology by intravascular ultrasonography and high-resolution MR imaging are new imaging modalities that have been used to characterize plaque morphology and composition in peripheral arteries.

MATERIALS AND METHODS: The objectives of this study were 1) to determine the correlation between virtual histology–intravascular ultrasonography and histopathologic analysis (reference standard) and 2) to explore the comparative results of 7T MR imaging (versus histopathologic analysis), both to be performed in vitro by use of intracranial arterial segments with atherosclerotic plaques. Thirty sets of postmortem samples of intracranial circulation were prepared for the study. These samples included the middle cerebral artery ($n = 20$), basilar artery ($n = 8$), and anterior cerebral artery ($n = 2$). Virtual histology–intravascular ultrasonography and 7T MR imaging were performed in 34 and 10 points of interest, respectively. The formalin-fixed arteries underwent tissue processing and hematoxylin-eosin staining. The plaques were independently categorized according to revised Stary classification after review of plaque morphology and characteristics obtained from 3 modalities. The proportion of fibrous, fibrofatty, attenuated calcium, and necrotic components in the plaques were determined in histology slides and compared with virtual histology–intravascular ultrasonography and MR imaging.

RESULTS: Of 34 points of interest in the vessels, 32 had atherosclerotic plaques under direct visualization. Plaques were visualized in gray-scale intravascular ultrasonography as increased wall thickness, outer wall irregularity, and protrusion. The positive predictive value of virtual histology–intravascular ultrasonography for identifying fibroatheroma was 80%. Overall, virtual histology–intravascular ultrasonography accurately diagnosed the type of the plaque in 25 of 34 samples, and κ agreement was 0.58 (moderate agreement). The sensitivity and specificity of virtual histology–intravascular ultrasonography readings for fibroatheroma were 78.9% and 73.3%, respectively. The overall sensitivity and specificity for virtual histology–intravascular ultrasonography were 73.5% and 96.6%, respectively. Plaques were identified in 7T MR imaging as increased wall thickness, luminal stenosis, or outer wall protrusion. The positive predictive value of 7T MR imaging for detecting fibrous and attenuated calcium deposits was 88% and 93%, respectively.

CONCLUSIONS: This in vitro study demonstrated that virtual histology–intravascular ultrasonography and high-resolution MR imaging are reliable imaging tools to detect atherosclerotic plaques within the intracranial arterial wall, though both imaging modalities have some limitations in accurate characterization of the plaque components. Further clinical studies are needed to determine the clinical utility of plaque morphology and composition assessment by noninvasive tests.

ABBREVIATIONS: IVUS = intravascular ultrasonography; SPACE = sampling perfection with application-optimized contrasts by use of different flip angle evolutions; VH = virtual histology

Intracranial atherosclerotic disease accounts for up to 10% of ischemic strokes.[1] Recent studies suggest that imaging of plaque burden, composition, and morphology provides additional insight regarding the risk of thrombo-embolism and response to endovascular treatment in coronary and carotid artery plaques.[2] The consensus conference on intracranial atherosclerotic disease in 2009 identified plaque characterization as an important method of identification for patients with intracranial atherosclerotic disease who are at risk for ischemic events.[3] Intravascular ultrasonography (IVUS) and high-resolution MR imaging are gaining prominence in the imaging of characteristics of atherosclerotic plaques.[4-6] Despite numerous studies regarding the use of these modalities in coronary and carotid arteries, such data are lacking in intracranial arteries and atherosclerotic plaques. Intra-

Received February 13, 2013; accepted after revision March 26, 2013.

From the Zeenat Qureshi Stroke Research Center (S.M., M.W., A.E.H., M.F.K.S., A.I.Q.), Center for Magnetic Resonance Research (J.S., P.-F.V.d.M.), and Department of Laboratory Medicine and Pathology (H.B.C.), University of Minnesota, Minneapolis, Minnesota.

Please address correspondence to Shahram Majidi, MD, Zeenat Qureshi Stroke Research Center, University of Minnesota, 420 Delaware St SE, MMC 295, Minneapolis, MN 55455; e-mail: drsmajidi@gmail.com

http://dx.doi.org/10.3174/ajnr.A3631

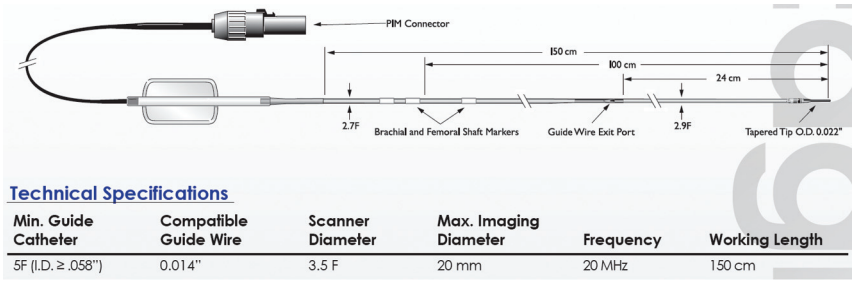

FIG 1. Characteristics of Eagle Eye Gold IVUS imaging catheter.

cranial arteries have unique features including a smaller wall-to-lumen ratio, thinner wall thickness, and thinner intima compared with coronary and carotid arteries.[7,8]

In this study, we evaluated the ability of virtual histology (VH) by IVUS to identify intracranial plaque characteristics compared with histopathologic analysis. Additional imaging data were collected on a 7T scanner in a subset of the samples to evaluate lesion detection capability on the basis of very high spatial resolution MR images.

MATERIALS AND METHODS

The study protocol was reviewed and approved by the Anatomy Bequest Program at the University of Minnesota, Minneapolis. Ten human cadaver brains were inspected for selection of intracranial vessels with atherosclerotic plaques. A total of 30 different vessels including 8 basilar and 20 middle and 2 anterior cerebral arteries were selected for the study. The vessels were preserved in formalin for 8 weeks before the study. Decalcification was not performed before sectioning.

Virtual Histology by IVUS

The vessel specimens were pinned on a gel by use of metal needles in a dissecting tray filled with normal saline at room temperature. The proximal and distal ends of each vessel were connected to a 6F catheter to allow flushing of the artery during the IVUS imaging. The 20-MHz IVUS catheter (Eagle Eye Gold, 20 MHz Digital, 64 Bement, s5 Imaging System; Volcano Corporation, Rancho Cordova, California) was then inserted into the vessel lumen and advanced beyond the atherosclerotic portion of the vessel. The IVUS signal derated intensity, spatial peak temporal average ($I_{SPTA.3}$), was 2.68 (mW/cm^2), with a maximum scanning diameter of the catheter of 20 mm (set at 10 mm during the experiment) (Fig 1). An electrocardiogram simulator (60 beats per minute) was connected to the system to enable the VH data acquisition. The IVUS catheter was then slowly pulled back by use of the catheter pullback device (Trak Back II; Volcano Corporation) at a speed of 0.5 mm/s. VH-IVUS data analysis was performed by an independent expert blinded to the baseline lesion characteristics. Percentages of the 4 different components of plaques were identified within the color-coded map on VH-IVUS as described below[9]:

1) Fibrous tissue: area of densely packed collagen (dark green component).

2) Fibrofatty tissue: area of collagen fibers with high lipid accumulation (light green component).

3) Necrotic tissue: area with high content of lipid, foam cells, and necrotic cells (red component).

4) Dense calcium: areas with compact calcium deposit without presence of necrosis (white component).

The plaques were also classified to 1 of the 6 categories of atherosclerotic plaque on the basis of a previously published classification[10]:

1) Pathologic intimal thickening: intima media thickness >300 μm, fibrofatty component >10%, necrotic core and calcium amount <10% of plaque area; 2) fibroatheroma: necrotic core >10% of plaque area; 3) calcified fibroatheroma: fibroatheroma with areas of calcium deposition; 4) thin-cap fibroatheroma: necrotic core confluent against the lumen with >10% of plaque area; 5) calcified thin-cap fibroatheroma: areas of calcium deposition in thin-cap fibroatheroma plaque; or 6) fibrocalcific: calcium deposition >10% of plaque area; fibrofatty and necrotic core comprise <10% of plaque.

High-Resolution 7T MR Imaging

First, vessel specimens were placed between 2 plastic plates with a spacer between the plates immersed in a rectangular box (125 × 98 × 3 mm^3) filled with Fomblin (perfluoropolyether; Ausimont, Morristown, New Jersey). Fomblin does not have water protons; thus, only signal from the specimen was measured in MR imaging.[11] The MR images were acquired on a 7T magnet (Magnex Scientific, Oxford, United Kingdom) driven with a Magnetom 7T console (Siemens Erlangen, Germany). A volume coverage head coil (16 transceiver channels) was used for excitation and reception, as previously described.[12] To improve signal-to-noise ratio, signal was also received on a home-built preamplifier-decoupled (Microwave Technology, Fremont, California) 2-loop receiver coil (5 cm each) made of 12-gauge silver-plated copper wire on which the sample box was directly positioned. In preliminary experiments with multi-echo and multi-inversion-recovery time sequences, average relaxation time T2 and T1 values of the vessel walls at 7T were estimated to be ~35 ms and ~1400 ms, respectively. Ex vivo 3D images were obtained by means of the 3D sampling perfection with application-optimized contrasts by use of different flip angle evolutions (SPACE) sequence,[13] with the following parameters: TR/TE = 3000/60 ms, FOV = 95 × 119 × 10.4 mm, echo-train length = 14, generalized autocalibrating partially parallel acquisition acceleration factor = 2. Scan duration was 7 hours, 33 minutes; voxel size = 0.13 mm^3. 3D SPACE contrast is a combination of T1 and T2 contrast. The sequence parameters were chosen to provide a mixed contrast of T1 and T2 weight, dominated by T1 weight.

Histopathology

Formalin-fixed arterial specimens were cut into 4-mm sections and embedded in paraffin. Small sutures were placed in the arterial wall by use of 4–0 Prolene polypropylene suture (Ethicon, Somerville, New Jersey) and used as markers to enable matching the points of interest in IVUS and MR imaging with corresponding sections on histology. Subsequently, 6-μm sections were taken from the tissue blocks and stained with hematoxylin-eosin.

Table 1: Comparison of different types of atherosclerotic plaques between VH-IVUS and histologic sections (as reference standard)

Category of Plaque	Plaque Classification by Histological Analysis	Plaque Classification by VH-IVUS Analysis							
		True-Positive	True-Negative	False-Positive	False-Negative	Sensitivity	Specificity	PPV	NPV
No plaque	2	2	32	0	0	100	100	100	100
Pathologic intima thickening	6	3	28	0	3	50	100	100	90.3
Fibroatheroma	19	15	11	4	4	78.9	73.3	78.9	73.3
Calcified fibroatheroma[a]	0	0	33	1	0	0	97	0	100
Thin-cap fibroatheroma	3	2	30	1	1	66.6	96.7	66.6	96.7
Calcified thin-cap fibroatheroma	2	1	31	1	1	50	96.8	50	96.8
Fibrocalcific atheroma	2	2	32	0	0	100	100	100	100
Total	34	25	197	7	9	73.5	96.6	78.1	95.6

PPV indicates positive predictive value; NPV, negative predictive value.

[a] Number is small and requires cautious interpretation of false-positive or false-negative values.

Table 2: Area of 4 different components of plaque types in histologic sections and VH-IVUS analyses

	Histopathology, % (SD)	VH-IVUS, % (SD)	Pearson Correlation
Fibrous	45.6 (18.7)	50.8 (17.1)	0.66
Fibrofatty	35.6 (14.1)	12.5 (12.1)	0.34
Dense calcium	7.1 (7.6)	9.1 (5.2)	0.64
Necrosis	5.1 (4.6)	20.9 (10.9)	0.23

Histology slides were then reviewed by a neuropathologist who was blinded to the VH-IVUS and MR imaging data. The plaques were classified to one of the categories of atherosclerotic plaques types, based on the classification mentioned above.

Finally, histology slides were photographed under the microscope, and the area (mm^2) of different components of the plaques including fibrous, fibrofatty, attenuated calcium, and necrosis were quantitatively measured with the use of the manual segmentation tools of Analyze software (AnalyzeDirect, Overland Park, Kansas) as described previously.[14,15] For calculating the area by use of Analyze software, the ROI was manually selected for each component. The total amount of each component was then calculated by summing all the ROIs for that component by use of the "sample option" function.

Statistical Analysis

Statistical analyses were performed with the use of SAS software version 9.1 (SAS Institute, Cary, North Carolina). Kappa agreement, sensitivity and specificity, and positive and negative predictive values for VH-IVUS to identify different types of plaques[10] were calculated by use of classification on the basis of histologic findings as the reference standard (plaque categorization analysis). The positive and negative predictive values for VH-IVUS and MR images in identifying different plaque categories and fibrous and attenuated calcium components in the plaque were calculated using quantification on the basis of histologic findings as the reference standard (individual plaque component analysis). The correlation between areas (mm^2) of various components measured by histology and by VH-IVUS images was also calculated. Finally, the overall sensitivity and specificity for VH-IVUS reading in accurately characterizing plaque type with the actual histologic findings were calculated using the total numbers of true and false identification with VH-IVUS. Spatially matched cross-sectional MR images of the arteries with their corresponding histologic sections and VH-IVUS images were studied to determine positive and negative predictive values.

RESULTS

A total of 30 intracranial arterial segments (34 histologic sections) were examined by both VH-IVUS and microscopy of histologic sections. In exploratory analysis, 10 of the 30 intracranial arterial segments were also examined by 7T MR imaging.

Correlation Between VH-IVUS and Histopathologic Analysis

In the plaque categorization analysis, VH-IVUS was able to detect the presence of atherosclerotic plaque in all specimens with morphologically visible abnormalities and absence of plaque in 2 specimens without atherosclerotic plaque by histology. VH-IVUS identification of plaque type correlated with histology sections analysis in 25 of 34 specimens (κ agreement was 0.58). The most frequent type of the plaques by histology was fibroatheroma, and VH-IVUS identification correlated with histology analysis in 15 of 19 corresponding points of interest within arteries (positive and negative predictive values of VH-IVUS were 78.9% and 73.3%, respectively). The sensitivity and specificity of VH-IVUS readings for fibroatheroma were 78.9% and 73.3%, respectively. As shown in Table 1, the overall sensitivity and specificity for VH-IVUS were 73.5% and 96.6%, respectively. Fig 2 demonstrates 2 samples of histology slides with their corresponding VH-IVUS images.

In the individual plaque component analysis, positive and negative predictive values of VH-IVUS to identify the presence of calcium in atherosclerotic plaque were 50% and 100%, respectively. Regarding the presence of necrosis, VH-IVUS had the positive and negative predictive values of 97% and 67%, respectively, for identifying necrosis. The quantitative proportions of different plaque components (fibrous, fibrofatty, necrosis, and attenuated calcium) were also measured in histology sections and compared with VH-IVUS images. Overall, fibrous component was the most frequent component of the plaques both in histologic sections and VH-IVUS imaging study. As shown in Table 2, the area of fibrous component and attenuated calcium deposits had the highest rates of correlation between histology and VH-IVUS images (Pearson correlations of 0.66 and 0.64, respectively).

Correlation Between 7T MR Imaging and Histopathologic Analysis

MR imaging was successfully performed in 10 different points of interest including 3 basilar and 7 middle cerebral arterial segments. An increased wall thickness was detected by MR imaging in all sites in which plaques were identified in histologic sections.

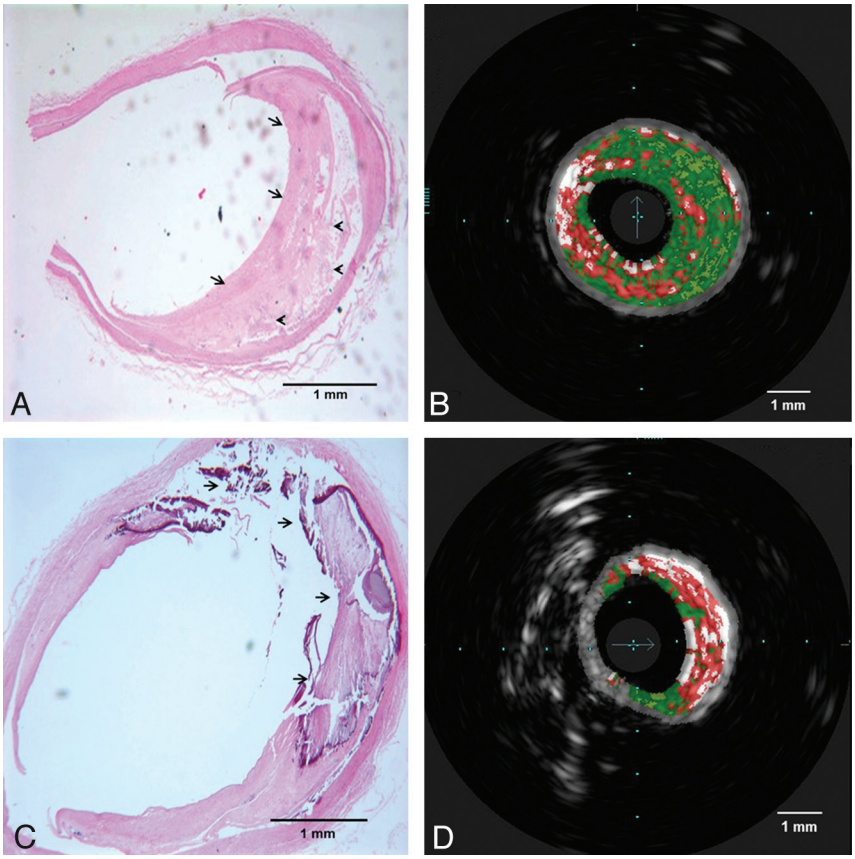

FIG 2. Histopathologic sections with corresponding VH-IVUS images. *A* and *B,* Fibrous (*arrows* in *A*) and fibrofatty (*arrowheads* in *A*) tissues in the histologic section are correlated with dark green and light green areas in VH-IVUS, respectively. *C* and *D,* attenuated calcium and necrotic area (*arrows* in *C*) and its corresponding area in VH-IVUS red (necrosis) and white (attenuated calcium) areas.

In a more detailed analysis of individual plaque components within each lesion, the fibrotic components were identified as areas of hyperintense signal in 3D SPACE MR images, whereas areas of attenuated calcium deposition were identified as areas of hypointense signal in the same image. Note that the SPACE MR imaging sequence provided a mixed contrast, combining T1 and T2 weights (Fig 3).

DISCUSSION

As a result of compensatory dilation (remodeling), vessel wall thickening related to intracranial atherosclerosis may not cause proportional luminal narrowing.[16,17] Therefore, imaging modalities such as conventional angiography and CT angiography, which are based on detecting severity of luminal narrowing, may underestimate the severity and subsequent risk of ischemic events of intracranial atherosclerotic disease.

In this study focusing on intracranial arteries, VH-IVUS and 7T MR imaging were able to detect all of the atherosclerotic plaques as increased wall thickness. Normal vessels were visualized as vessels with no irregularity and/or thickness change in the wall, in both VH-IVUS and MR imaging. There was a moderate agreement (κ agreement of 0.58) between VH-IVUS and actual histologic evaluation in plaque categorization analysis. Considering all types of plaque, the overall sensitivity and specificity for VH-IVUS were 73.5% and 96.6%, respectively. We also validated the accuracy of high-resolution MR imaging and VH-IVUS for detecting fibrous content and attenuated calcium deposits. VH-IVUS had high yield for detection and quantitation of fibrous area and attenuated calcium deposits.

However, VH-IVUS underestimated the quantitative estimates of necrotic core and fibrofatty areas, which are limitations previously noted in analyses of coronary arteries.[18-20] The relative lack of identification of necrotic core can be partly explained by the different definitions used in histologic analysis and VH-IVUS.[21] In histologic analysis, the necrotic core is defined by areas with lipid-rich cellular debris and lack of extracellular matrix[22,23]; VH-IVUS relies on the presence of calcification to detect the necrotic core.[9,24] Moreover, the current resolution of VH-IVUS (100–200 mm) is not high enough to detect thin-cap fibroatheroma and necrotic core.[25] To obtain greater accuracy, the use of contrast-enhanced ultrasonography, high-resolution MR imaging, multidetector CT, and concurrent VH-IVUS may be required.[2,26,27]

VIVA (VH-IVUS in Vulnerable Atherosclerosis)[28] and PROSPECT (Providing Regional Observations to Study Predictors of Events in the Coronary Tree)[29] are 2 prospective studies that demonstrated that VH-IVUS can reliably identify the atherosclerotic plaques that are at increased risk of major adverse cardiac events. The unique features of intracranial vessels prevent extrapolation of current data regarding plaque characterization by use of different imaging modalities in extracranial vessels. Intracranial arteries have a smaller wall-to-lumen ratio, thinner wall thickness, and thinner intima compared with coronary and carotid arteries. In comparison to extracranial vessels, the intracranial vessels have a more prominent internal elastic layer and less advanced adventitia and media.[30] Only preliminary data regarding the clinical application of plaque characterization are available. Preliminary data suggest the existence of a nonatherosclerotic variant involving the anterior circulation that may be prone to high rates of restenosis after stent treatment.[31,32] However, angiography is unable to differentiate nonatherosclerotic from atherosclerotic disease and assess the burden of fibrosis within plaque. Therefore, plaque differentiation may be valuable in assessing the risk-benefit ratio of medical and endovascular treatment options.

The use of VH-IVUS is limited as an adjunct to an invasive procedure such as cerebral angiogram, intracranial angioplasty, or stent placement and is possible in selected proximal arteries without excessive tortuosity. The new generations of VH-IVUS

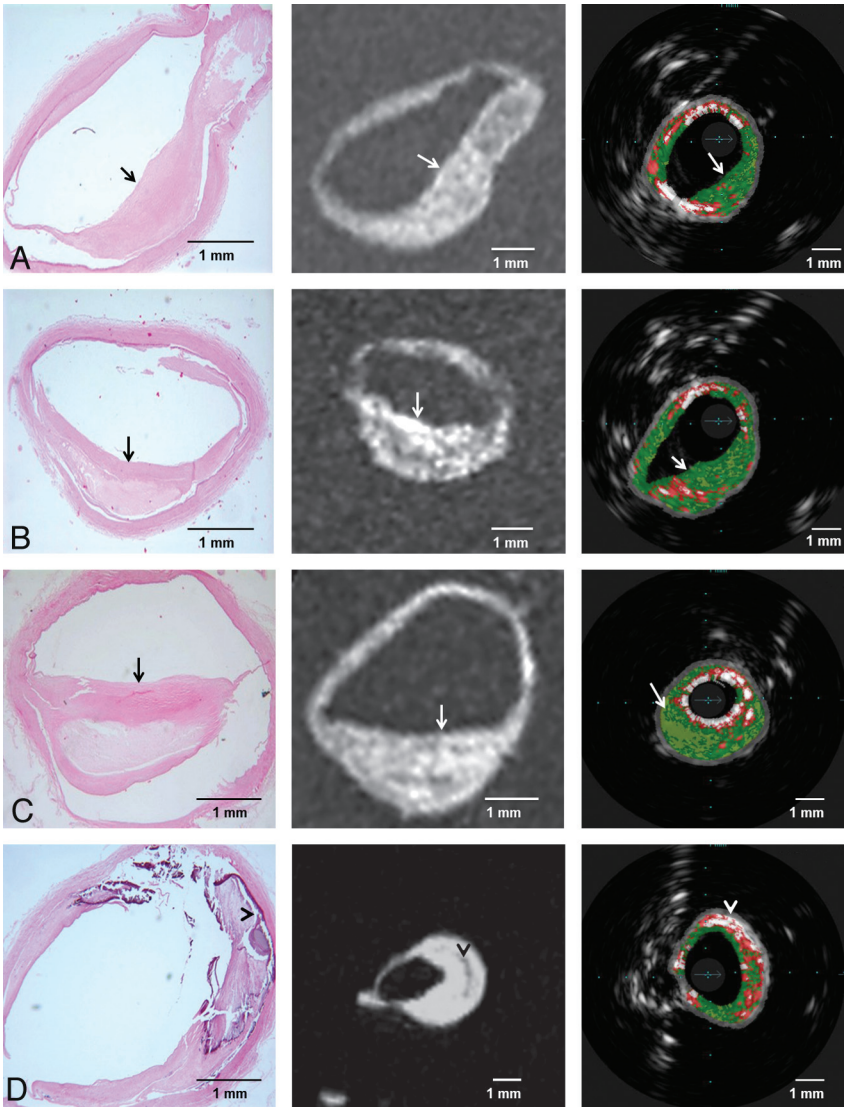

FIG 3. Four different histopathologic sections of intracranial vessels with atherosclerotic plaque and their corresponding 3D SPACE MR imaging (in the middle) and VH-IVUS (on the right) images. Fibrous areas (*arrows*) and attenuated calcium (*arrowheads*) consistently visualized as areas with hyperintense and hypointense signals in MR imaging, respectively.

catheters are expected to be more flexible, with a smaller profile, which would allow passage of these catheters through the tortuous intracranial arteries; henceforth, such imaging is expected to gain greater use in neuro-endovascular procedures.[33]

Regarding the MR imaging component of our experiment, we aimed to study the value of high-resolution MR imaging as a secondary or exploratory aim. Although the acquisition time of these initial MR imaging results was far beyond any affordable in vivo scan duration, we deliberately chose to benefit from the in vitro nature of the study to first determine whether plaque lesions could—at all—be imaged with the SPACE sequence at 7T MR imaging by use of a very high spatial resolution (voxel size approximately 500 times smaller than 1 mm^3). The positive results reported here provide a strong rationale to further optimize MR acquisition protocols by use of lower spatial resolution, toward a trade-off, providing acceptable acquisition time while preserving plaque detectability. Further in vivo studies will also be necessary to determine the sensitivity of such acquisitions to physiologic motion.

The experimental MR imaging setup (spatial extent of sensitivity of the coils smaller than in vitro specimens) and the length and alignment of arterial segments available for imaging prevented us from acquiring adequate 7T MR imaging in all plaques. We acknowledge that the relatively small sample size may not allow an adequate quantitative analysis of the value of high-resolution MR imaging in characterizing plaque categories.

Our study has several limitations. First, VH-IVUS and MR imaging were performed in in vitro settings with specimens fixed in formalin. The tissue handling and processing may induce some artifact in the size and morphology of the plaques. These changes may affect the generalization of the results to practical clinical settings. In vitro settings are appropriate for validation studies of VH-IVUS before clinical application.[9,18] Our sample size for some types of the plaques and negative sites (none atherosclerotic vessel) was very small, which requires cautious interpretation of the estimates for each of the plaque types separately.

CONCLUSIONS

This study demonstrated that VH-IVUS and 7T MR imaging are reliable imaging modalities to detect atherosclerotic plaques and to quantify plaque burden within the intracranial arterial wall. Both imaging modalities have some limitations in accurate classification of plaque type and characterization of the plaque components. The application of these imaging techniques may provide additional risk stratification in regard to ischemic events and lesion progression in patients with intracranial atherosclerotic disease.

Disclosures: Ameer Hassan—*UNRELATED: Payment for lectures (including service on speakers bureaus):* MicroVention, Comments: Honorarium. Pierre-Francois Van de Moortele—*RELATED: Grant:* NIH.* Muhammad Suri—*RELATED: Grant:* NIH, Comments: NIH K12 award; *Support for travel to meetings for the study or other purposes:* NIH, Comments: NIH K12 award. Adnan Qureshi—*UNRELATED: Consultancy:* Cornerstone Therapeutics Adnan I. Qureshi is supported by the National Institute of Neurological Diseases and Stroke. Principal Investigator, Antihypertensive Treatment in Acute Cerebral Hemorrhage (ATACH)-II. 1U01NS062091 (medication provided by EKR therapeutics) and the American Heart Association Established Investigator Award 0840053 N, Innovative Strategies for Treating Cerebral Hemorrhage. (**money paid to institution*).

REFERENCES

1. Kasner SE, Chimowitz MI, Lynn MJ, et al. **Predictors of ischemic stroke in the territory of a symptomatic intracranial arterial stenosis.** *Circulation* 2006;113:555–63

2. Yuan C, Mitsumori LM, Beach KW, et al. **Carotid atherosclerotic plaque: noninvasive MR characterization and identification of vulnerable lesions.** *Radiology* 2001;221:285–99
3. Qureshi AI, Feldmann E, Gomez CR, et al. **Consensus conference on intracranial atherosclerotic disease: rationale, methodology, and results.** *J Neuroimaging* 2009;19(Suppl 1):1S–10S.
4. Nair A, Calvetti D, Vince DG. **Regularized autoregressive analysis of intravascular ultrasound backscatter: improvement in spatial accuracy of tissue maps.** *IEEE Trans Ultrason Ferroelectr Freq Control* 2004;51:420–31
5. van der Kolk AG, Zwanenburg JJ, Brundel M, et al. **Intracranial vessel wall imaging at 7.0-T MRI.** *Stroke* 2011;42:2478–84
6. Zacharatos H, Hassan AE, Qureshi AI. **Intravascular ultrasound: principles and cerebrovascular applications.** *AJNR Am J Neuroradiol* 2010;31:586–97
7. Walmsley JG, Canham PB. **Orientation of nuclei as indicators of smooth muscle cell alignment in the cerebral artery.** *Blood Vessels* 1979;16:43–51
8. Walmsley JG. **Vascular smooth muscle orientation in straight portions of human cerebral arteries.** *J Microsc* 1983;131:361–75
9. Nair A, Kuban BD, Tuzcu EM, et al. **Coronary plaque classification with intravascular ultrasound radiofrequency data analysis.** *Circulation* 2002;106:2200–06
10. Diethrich EB, Pauliina Margolis M, Reid DB, et al. **Virtual histology intravascular ultrasound assessment of carotid artery disease: the Carotid Artery Plaque Virtual Histology Evaluation (CAPITAL) study.** *J Endovasc Ther* 2007;14:676–86
11. Benveniste H, Kim K, Zhang L, et al. **Magnetic resonance microscopy of the C57BL mouse brain.** *NeuroImage* 2000;11:601–11
12. Adriany G, Van de Moortele PF, Ritter J, et al. **A geometrically adjustable 16-channel transmit/receive transmission line array for improved RF efficiency and parallel imaging performance at 7 Tesla.** *Magn Reson Med* 2008;59:590–97
13. Mugler JP III, Brookeman JR. **Efficient spatially-selective single-slab 3D turbo-spin-echo imaging.** *The International Society for Magnetic Resonance in Medicine (ISMRM)* Twelve Scientific Meeting and Exhibition, May, 15–21, 2004. Kyoto, Japan. [Abstract: 695]
14. Zimmerman RD, Maldjian JA, Brun NC, et al. **Radiologic estimation of hematoma volume in intracerebral hemorrhage trial by CT scan.** *AJNR Am J Neuroradiol* 2006;27:666–70
15. Divani AA, Majidi S, Luo X, et al. **The ABCs of accurate volumetric measurement of cerebral hematoma.** *Stroke* 2011;42:1569–74
16. Glagov S, Weisenberg E, Zarins CK, et al. **Compensatory enlargement of human atherosclerotic coronary arteries.** *N Engl J Med* 1987;316:1371–75
17. Ma N, Jiang WJ, Lou X, et al. **Arterial remodeling of advanced basilar atherosclerosis: a 3-Tesla MRI study.** *Neurology* 2010;75:253–58
18. Hishikawa T, Iihara K, Ishibashi-Ueda H, et al. **Virtual histology-intravascular ultrasound in assessment of carotid plaques: ex vivo study.** *Neurosurgery* 2009;65:146–52
19. Obaid DR, Calvert PA, McNab D, et al. **Identification of coronary plaque sub-types using virtual histology intravascular ultrasound is affected by inter-observer variability and differences in plaque definitions.** *Circ Cardiovasc Imaging* 2012;5:86–93
20. Timaran CH, Rosero EB, Martinez AE, et al. **Atherosclerotic plaque composition assessed by virtual histology intravascular ultrasound and cerebral embolization after carotid stenting.** *J Vasc Surg* 2010;52:1188–94
21. Thim T, Hagensen MK, Wallace-Bradley D, et al. **Unreliable assessment of necrotic core by virtual histology intravascular ultrasound in porcine coronary artery disease.** *Circ Cardiovasc Imaging* 2010;3:384–91
22. Mann J, Davies MJ. **Mechanisms of progression in native coronary artery disease: role of healed plaque disruption.** *Heart* 1999;82:265–68
23. Burke AP, Joner M, Virmani R. **IVUS-VH: a predictor of plaque morphology?** *Eur Heart J* 2006;27:1889–90
24. Nair A, Kuban BD, Obuchowski N, et al. **Assessing spectral algorithms to predict atherosclerotic plaque composition with normalized and raw intravascular ultrasound data.** *Ultrasound Med Biol* 2001;27:1319–31
25. Nakazawa G, Finn AV, Virmani R. **Virtual histology: does it add anything?** *Heart* 2007;93:897–98
26. Vancraeynest D, Pasquet A, Roelants V, et al. **Imaging the vulnerable plaque.** *J Am Coll Cardiol* 2011;57:1961–79
27. Yuan C, Mitsumori LM, Ferguson MS, et al. **In vivo accuracy of multispectral magnetic resonance imaging for identifying lipid-rich necrotic cores and intraplaque hemorrhage in advanced human carotid plaques.** *Circulation* 2001;104:2051–56
28. Calvert PA, Obaid DR, O'Sullivan M, et al. **Association between IVUS findings and adverse outcomes in patients with coronary artery disease: the VIVA (VH-IVUS in Vulnerable Atherosclerosis) Study.** *JACC Cardiovasc Imaging* 2011;4:894–901
29. Stone GW, Maehara A, Lansky AJ, et al. **A prospective natural-history study of coronary atherosclerosis.** *N Engl J Med* 2011;364:226–35
30. Merei FT, Gallyas F, Horvath Z. **Elastic elements in the media and adventitia of human intracranial extracerebral arteries.** *Stroke* 1980;11:329–36
31. Siddiq F, Chaudhry SA, Vazquez G, et al. **Intracranial stenosis in young patients: unique characteristics and risk factors.** *Neuroepidemiology* 2012;38:148–53
32. Qureshi AI, Feldmann E, Gomez CR, et al. **Intracranial atherosclerotic disease: an update.** *Ann Neurol* 2009;66:730–38
33. Takayama K, Taoka T, Nakagawa H, et al. **Successful percutaneous transluminal angioplasty and stenting for symptomatic intracranial vertebral artery stenosis using intravascular ultrasound virtual histology.** *Radiat Med* 2007;25:243–46